



A Suppressor/Avirulence Gene Combination in *Hyaloperonospora arabidopsidis* Determines Race Specificity in *Arabidopsis thaliana*

Alison Woods-Tör¹, David J. Studholme², Volkan Cevik³, Osman Telli¹, Eric B. Holub⁴ and Mahmut Tör^{1*}

¹ Institute of Science and the Environment, University of Worcester, Worcester, United Kingdom, ² College of Life and Environmental Sciences, University of Exeter, Exeter, United Kingdom, ³ Department of Biology and Biochemistry, University of Bath, Bath, United Kingdom, ⁴ Warwick Crop Centre, School of Life Sciences, University of Warwick, Coventry, United Kingdom

OPEN ACCESS

Edited by:

Xin Li,
University of British Columbia, Canada

Reviewed by:

Daolong Dou,
Nanjing Agricultural University, China
Hugo Germain,
Université du Québec à Trois-Rivières,
Canada

*Correspondence:

Mahmut Tör
m.tor@worc.ac.uk

Specialty section:

This article was submitted to
Plant Microbe Interactions,
a section of the journal
Frontiers in Plant Science

Received: 15 December 2017

Accepted: 14 February 2018

Published: 01 March 2018

Citation:

Woods-Tör A, Studholme DJ, Cevik V,
Telli O, Holub EB and Tör M (2018) A
Suppressor/Avirulence Gene
Combination in *Hyaloperonospora
arabidopsidis* Determines Race
Specificity in *Arabidopsis thaliana*.
Front. Plant Sci. 9:265.
doi: 10.3389/fpls.2018.00265

The pathosystem of *Arabidopsis thaliana* and diploid biotrophic oomycete *Hyaloperonospora arabidopsidis* (*Hpa*) has been a model for investigating the molecular basis of Flor's gene-for-gene hypothesis. The isolates *Hpa*-Noks1 and *Hpa*-Cala2 are virulent on *Arabidopsis* accession RMX-A02 whilst an F₁ generated from a cross between these two isolates was avirulent. The F₂ progeny segregated 3,1 (avirulent, virulent), indicating a single major effect AVR locus in this pathogen. SNP-based linkage mapping confirmed a single AVR locus within a 14 kb map interval containing two genes encoding putative effectors. The *Hpa*-Cala2 allele of one gene, designated *H. arabidopsidis cryptic1* (*HAC1*), encodes a protein with a signal peptide and an RxLR/dEER motif, and triggers a defense response in RMX-A02. The second gene is heterozygous in *Hpa*-Cala2. One allele, designated *Suppressor of HAC1^{Cala2}* (*S-HAC1^{Cala2}*) encodes a protein with a signal peptide and a dKEE motif with no RxLR motif; the other allele (*s-hac1^{Cala2}*) encodes a protein with a signal peptide, a dEEE motif and is divergent in sequence from the *S-HAC1^{Cala2}* allele. In selfed progeny from *Hpa*-Cala2, dominant *S-HAC1^{Cala2}* allele carrying progeny correlates with virulence in RMX-A02, whereas homozygous recessive *s-hac1^{Cala2}* carrying progeny were avirulent. Genetic investigations suggested other heterozygous suppressor loci might exist in the *Hpa*-Cala2 genome.

Keywords: effector, avirulence inhibitor, suppressor, oomycete, *Arabidopsis*, downy mildew, heterozygosity

INTRODUCTION

Oomycetes are diploid microorganisms that resemble fungi in morphology and lifestyle, having filamentous mycelia and developing specialized structures such as haustoria during infection. However, they are taxonomically distinct from fungi and are instead placed within the Stramenopiles (Keeling et al., 2005). Oomycetes contain several economically important crop pathogens including *Phytophthora infestans* (tomato and potato late blight), *P. ramorum* (sudden oak death), *Plasmopora viticola* (grapevine downy mildew), *Pythium ultimum* (damping off and root rot), *Bremia lactuca* (lettuce downy mildew), and *Albugo candida* (white blister rust of crucifers) (Kamoun et al., 2015).

The biotrophic oomycete *Hyaloperonospora arabidopsidis* (*Hpa*, formerly known as *H. parasitica*) has co-evolved as a downy mildew pathogen in wild populations of *Arabidopsis thaliana* (Göker et al., 2004; Holub, 2006), and has been used for more than 25 years as an experimental model (Koch and Slusarenko, 1990; Tör et al., 1994) for investigating the molecular basis of the gene-for-gene theory proposed by H. H. Flor to explain genetic evidence that for each gene controlling resistance in the host, there is a corresponding gene controlling pathogenicity in the pathogen (Flor, 1946). At least seven downy mildew *R*-genes have been characterized in this pathosystem (Botella et al., 1998; McDowell et al., 1998; Bittner-Eddy et al., 1999; van der Biezen et al., 2002; Sinapidou et al., 2004; Eulgem et al., 2007), and all encode cytoplasmic NLR proteins that contain a conserved nucleotide-binding site (NBS) and a variable leucine-rich repeat (LRR) domain. Three of the seven predicted AVR elicitors have also been characterized (Allen et al., 2004; Rehmany et al., 2005; Bailey et al., 2011) and all encode secreted effector-like proteins.

Plant pathogens deliver effectors to establish infection by suppressing the host immune system, altering plant physiology, and colonizing the host cell (Doehlemann and Hemetsberger, 2013; Win et al., 2013). Current consensus suggests that effectors target apoplastic and cytoplasmic components (Shan et al., 2008; Dodds and Rathjen, 2010; Pedersen et al., 2012). Fungal and oomycete pathogens secrete effectors with the involvement of an N-terminal signal peptide (Kamoun, 2006; Song et al., 2009), and some studies of oomycetes suggest that RxLR and dEER motifs may be involved in the translocation of these effectors into the host cell (Whisson et al., 2007; Tyler et al., 2013). However, a recent proteomic investigation on the RxLR effector AVR3a from the potato pathogen *P. infestans* demonstrated that the N-terminal part of the native protein up to and including the RxLR motif but excluding the dEER motif is cleaved off before the secretion, indicating a possible role of the RxLR motif in secretion of the effector from the pathogen (Wawra et al., 2017). Effectors that elicit a defense response due to detection by an R-protein are referred to as avirulence elicitor proteins (Jones and Dangl, 2006).

Interestingly, H. H. Flor described an exception to the simplified “gene-for-gene” model in which avirulent progeny of the flax rust fungus *Melampsora lini* were derived from sexual mating of two virulent isolates. He used selfing, back-crossing, and inter-mating of progeny to verify that several avirulence genes each had a matching suppressor/inhibitor gene. Lawrence et al. (1981) subsequently confirmed these results in the flax rust pathosystem. A similar example was described from detailed genetic studies in the rice blast fungus *Magnaporthe grisea* (Ellingboe, 1992; Lau et al., 1993). In some cases, the suppressor and the avirulent determinant were tightly linked on the same chromosome and could not be separated by recombination (Lau et al., 1993). Recent studies have begun to reveal the molecular basis of such interactions in other fungi. For example, Avr1 of *Fusarium oxysporum* f.sp. *lycopercisi* is recognized by the tomato *R*-gene product I-1 but suppresses the recognition of Avr2 and Avr3 by I-2 and I-3, respectively (Houterman et al., 2008). Current studies suggest that the suppressor/avirulence

gene combination provides the basis of specificity in fungi and oomycetes (Bourras et al., 2016).

Whilst genetic studies into *Arabidopsis-Hpa* interactions have shown the existence of a gene-for-gene relationship, molecular, and bioinformatics investigations have helped the cloning of several avirulent determinants in the pathogen and the corresponding *R*-genes in the host (Holub et al., 1994; Holub, 2006; Baxter et al., 2010; Bailey et al., 2011). Some of the *Hpa* RXLR-type effector proteins have been molecularly characterized. For example, ATR1 (Rehmany et al., 2005) is recognized by RPP1 by direct association via C-terminal leucine-rich repeats (Steinbrenner et al., 2015). ATR13 (Allen et al., 2004) is a highly polymorphic and dynamic protein with two surface-exposed patches of polymorphism, only one of which is involved in specific recognition of RPP13-Nd (Leonelli et al., 2011). ATR39-1 has been identified by computational methods and is recognized by RPP39 in *Arabidopsis* accession Weiningen (Wei-0) (Goritschnig et al., 2012). Recently we cloned ATR5^{Emoy2}, which does not have the RxLR motif but contains a dEER motif (Bailey et al., 2011). All of these *Hpa* effectors are avirulence determinants and, until now, no suppressor has been identified for any of them. Here, we report the genetic identification and map-based cloning of a *H. arabidopsidis* cryptic (*HAC1*^{Cala2}) avirulence determinant and a predicted matching suppressor (*S-HAC1*^{Cala2}) from the same interval using a sexual cross between two virulent isolates of *H. arabidopsidis*. *HAC1*^{Cala2} is an RxLR-dEER type putative effector protein inherited in progeny from the parent isolate *Hpa*-Cala2 and can trigger an immune response in the *A. thaliana* accession RMX-A02. *S-HAC1*^{Cala2} is in the same parent isolate within the genetic interval next to the *HAC1*^{Cala2} gene and encodes a putative effector protein with a dKEE motif. *S-HAC1*^{Cala2} is epistatic over *HAC1*^{Cala2}.

MATERIALS AND METHODS

Arabidopsis Germplasm

A. thaliana accessions Columbia (Col-0), Landsberg *erecta* (Ler-0) and a subset from the Nordborg-Bergelson collection (Nordborg et al., 2005) were used in this study. All can be obtained from the Nottingham Arabidopsis Stock Center (<http://arabidopsis.info>). Wassilewskija-*eds1.1* was described previously (Parker et al., 1996).

Pathogen Isolates and Pathology Methods

All isolates of *H. arabidopsidis* were maintained on *Ws-eds1* (Parker et al., 1996). Generation of a cross (CaNo F₁) between *Hpa*-Cala2 and *Hpa*-Noks1 was described previously (Bailey et al., 2011). Preparation of inoculum for experiments, and the assessment of sporulation were as described previously in Tör et al. (2002).

Bulk Segregant Analysis Using Next Generation Sequencing

Laboratory mating of *H. arabidopsidis* and production of CaNo F₂ isolates was described in our previous work (Bailey et al., 2011). The accession RMX-A02 was screened with 54 randomly

selected CaNo F₂ isolates. DNA was extracted separately from each individual F₂ isolate, and DNA from fifteen virulent (*hac1/hac1*) and fifteen avirulent (*HAC1/±*) F₂ isolates was pooled in equal concentrations to make up the virulent and avirulent bulks, respectively. One lane of 100 bp paired-end Illumina HiSeq2500 sequencing data was generated from each bulked pool, comprising 104 million reads for the virulent bulk and 110 million reads for the avirulent bulk. The Illumina reads were first trimmed based on their quality scores using Btrim (Kong, 2011) with a cut-off of 25 for average quality scores within a moving window of 5 bp. The minimum acceptable read length was 25 bp (that is, reads that were shorter than 25 bp after trimming were discarded). Other parameters for Btrim were set to default values. SPAdes v. 3.6.1; SSPACE v. 3.0 were then employed to *de novo* assemble both *Hpa-Cala2* and *Hpa-Noks1* genome sequences. We then Used BWA-mem to do the alignment of reads against the *Hpa-Noks1* genome assembly as a reference to map sequence reads from both virulent and avirulent bulks and the frequency of major allele at 26,722 sites have been examined. The contig 23137 (GenBank, LLKM01000918) had the highest percentage of SNP hit representing the largest difference between the bulks and used for subsequent mapping.

Map-Based Cloning of *HAC1* and *S-HAC1*

SNPs identified between the virulent and avirulent bulks using the genomic contig 23137 from *Hpa-Noks1* as a reference were converted to CAPS markers using dCAPS (<http://helix.wustl.edu/dcaps/dcaps.html>) (Neff et al., 2002). They were then used to map the *HAC1* locus. Once linkage was confirmed, flanking markers were used to identify the *Hpa-Emoy2* genomic Scaffold 41, and were also used for screening further F₂ isolates to identify recombinants. A total of 190 F₂ isolates were screened with the molecular markers. Recombinant CaNo F₂ isolates from either side of the interval were used to narrow the interval down to 14 kb on the Scaffold 41, 298,000–312,000. This region was checked on Ensembl Protist site (<http://protists.ensembl.org>) for possible ESTs. There were two gaps in the interval and both were filled manually by long PCR and sequencing the products. All PCR amplifications for mapping were performed in a total volume of 20 µl containing 20 ng of genomic DNA, forward and reverse primers (Supplemental Table 1) each at 0.2 µM, BioMix Red (Bioline). The PCR reaction consisted of a first step at 94°C for 3 min followed by 35 cycles of 30 s denaturation at 94°C, 30 s annealing at 50–60°C (based on T_m of primers) and 1 min extension at 72°C. Finally, an extension step was carried out at 72°C for 5 min. A 3 µl sample of each reaction volume was loaded onto a 1.5% agarose gel to ascertain whether PCR amplification was successful. The remaining 10–15 µl of PCR reactions were digested with relevant restriction enzymes following manufacturer's instructions. Digested products of PCR amplicons were separated on a 2% agarose gel containing TAE buffer at 110 V for 2 h, and visualized under UV light after staining with GelRed.

Expression Analysis

Total RNA was isolated from uninfected (control) or infected with *Hpa-Cala2*, *Hpa-Noks1*, *Hpa-Emoy2*, at 1, 2, 3, 4, 5, 6, and

7 day post inoculation (dpi) using RNeasy plant mini kit (Qiagen Ltd., West Sussex, UK) according to manufacturer's instructions. RT-PCR was performed with gene specific or *Hpa-Actin* primers (Supplemental Table 1), using 0.5 µg of total RNA as template. The PCR product was separated on a 1.5% agarose gel and stained with ethidium bromide. The products were verified by sequencing.

For quantitative RT-PCR, total RNA was isolated from *Ws-eds1* seedlings infected with *Hpa-Cala2* at 3, 4, and 7 dpi. Real-time PCR was carried out using gene specific primers for *HAC1^{Cala2}*, *S-HAC1^{Cala2}* and *s-hac1^{Cala2}*. The 10 µl reaction mix consisted of 40 ng of RNA, 5 µl SensiFAST Syber mix (SensiFAST™ SYBR® No-ROX One-Step Kit) 0.5 µM of each primer, 0.1 µl reverse transcriptase, 0.2 µl RNA inhibitor and DEPC water. PCR conditions were as follows, 45°C 20 min, 95°C for 2 min, followed by 10 cycles touchdown procedure; 95°C for 10 s, 1°C decrease in each annealing step of (68–59)°C for 15 s, 72°C 20 s; then 30 cycles of 95°C for 10 s, 59°C for 15 s 72°C for 20 s. PCR efficiency was detected as 98.7%. Relative abundance of *HAC1^{Cala2}*, *S-HAC1^{Cala2}*, and *s-hac1^{Cala2}* to *Hpa-Actin* was calculated as 2^{-ΔCt} (Livak and Schmittgen, 2001). Three samples were included for each analysis and the experiments were repeated three times.

RACE and DNA Sequencing

Total RNA was isolated from infected plant materials using RNeasy plant mini kit (Qiagen Ltd., West Sussex, UK) according to manufacturer's instructions. RACE was performed using the GeneRacer kit (Life Technologies Ltd, UK), following manufacturer's instructions using gene specific and nested primers (Supplemental Table 6). PCR regime and subsequent cloning was carried out as described by Bailey et al. (2011). PCR products or plasmid clones were sequenced using Mix2Seq Kit by Eurofins Genomics (Wolverhampton, UK).

Quantification of Pathogen Biomass and High-Resolution Melt Curve Analysis

Samples for genomic DNA isolation were collected from infected seedlings 7 dpi. Fifteen seedlings from each genotype made up a sample and three replicates were used for each sample. DNA was isolated using CTAB method (Doyle, 1987) and the PCR was performed in a total volume of 25 µl containing 50 ng of gDNA, 12.5 µl of SybrGreen Mastermix (ABI, Carlsbad, California), *Hpa-Actin* or *At-Actin* primers (Supplemental Table 1) and water on a Roche LightCycle 480 device. PCR conditions were as follows, 95°C for 4 min, then 10 cycles touchdown of 95°C for 30 s, annealing temperature of 65°C, decreasing 1°C every cycle to 56°C, and extension at 72°C for 30 s. After 10 cycles of touchdown, a further 25 cycles of 95°C for 30 s, 60°C for 30 s and 72°C for 30 s and a final extension at 72°C for 5 min were carried out. Relative abundance of *Hpa-Actin* to *At-Actin* was calculated as 2^{-ΔCt} (Livak and Schmittgen, 2001). High-resolution melt curve analysis (HRM) was carried out using gene specific primers for *s-hac1^{Cala2}* (Supplemental Table 1). The 20 µl reaction mix consisted of 30 ng of DNA, 10 µl HRM mix (Bioline Sensifast), 250 nM of each primer and sterile distilled water. PCR conditions were as follows, 95°C for 2 min, followed by 8 cycles of 95°C

for 5 s, 65°C for 10 s, 72°C 25 s; then 37 cycles of 95°C for 5 s, 58°C for 10 s 72°C for 25 s. This was followed by a melt cycle as follows, 95°C for 15 s, 40°C for 15 s, 70°C for 1 s, then increasing to 95°C with a ramp rate of 0.2°Cs⁻¹ with 25 fluorescence data acquisitions per °C.

Light Microscopy

Seedlings of infected and non-inoculated controls were stained with a solution of phenol, lactic acid, glycerol, and water (1,1,1,1) supplemented with 1 mg/ml trypan blue, decolourised in chloral hydrate and visualized under a compound microscope according to a previously described method (Koch and Slusarenko, 1990).

Agrobacterium-Mediated Transformation

Full-length *HAC1*, *S-HAC1*, and *s-hac1* candidate alleles were amplified from *Hpa-Cala2* and *Hpa-Noks1* genomic DNA using gene specific primers and cloned into pDONR/zeo vector (Life technologies) by Gateway cloning technology. Candidate genes were transferred to the binary vectors pEarleyGate100 (Earley et al., 2006) that has the constitutive 35S CMV promoter or pBAV150 (Vinatzer et al., 2006), which has Dexamethasone inducible promoter by LR recombination (Life technologies). The constructs were electroporated into *E. coli* strain DH10B and positive clones were identified by PCR and sequencing. The construct was then introduced into *Agrobacterium tumefaciens* strain GV3101 by electroporation and the RMX-A02 and Col-0 plants were transformed by the floral dip method (Clough and Bent, 1998). Transformants were selected by growing plants in soil soaked with 0.1% Basta (AgrEvo, Norfolk, UK) and inserts were confirmed by PCR using gene specific primers. Homozygous T₃ plants were obtained and used for the subsequent experiments.

Statistical Analysis

For statistical analysis, two-tailed students *t*-tests were performed on data obtained in plant infection assays and qRT-PCR.

Bioinformatics

IICB Genomics and Transcriptomics Resources (<http://eumicrobedb.org>) and EnsemblProtist (<http://protists.ensembl.org>) database were used for contig and EST information on *Hpa*. Several web servers, including InterPro (Quevillon et al., 2005) (<http://www.ebi.ac.uk/interpro/>), SMART (Letunic et al., 2012) (<http://smart.embl-heidelberg.de/>) and Pfam (Punta et al., 2012) (<http://pfam.xfam.org>) were used for the analysis of putative effector proteins. The *Hpa* genome (v8.3; <http://eumicrobedb.org/genome/>) was used to search for all possible ORFs, considering ATG as potential start codon. Web servers for SignalP V4.0 (Petersen et al., 2011) (<http://www.cbs.dtu.dk/services/SignalP/>) and TMHMM (Krogh et al., 2001) (<http://www.cbs.dtu.dk/services/TMHMM/>) were used to examine each ORFs for the presence of a signal peptide and transmembrane helices. Primer designs, *in silico* digests and comparison of genomic and full-length cDNA sequences of candidate genes were performed using Geneious (v8.0) (Kearse et al., 2012).

Accession Numbers

The raw sequence reads from the genomics sequencing of bulks are available from the Sequenced Read Archive (SRA) under accession numbers SRX1646609 (avirulent) and SRX1646555 (virulent). Genomic sequences of parental isolates can be found under accession numbers SRX1646645 for *Hpa-Cala2* and SRX1646646 for *Hpa-Noks1*. Accession numbers for the *HAC1* and *S-HAC1* alleles are KX523274, KX523275, KX523276, KX523277, KX523278, KX523279, and KX523280. Genome sequence assemblies for the parental isolates are available from GenBank under accession numbers LKIA00000000.1 and LLKM00000000.1 (Studholme and Tör, to be published elsewhere). Accession number of *Hpa-Noks1* 23137 contig is LLKM01000918. Accession number for *Hpa-Emoy2* reference genome v8.3 Scaffold 41 is ABWE00000000.2.

RESULTS

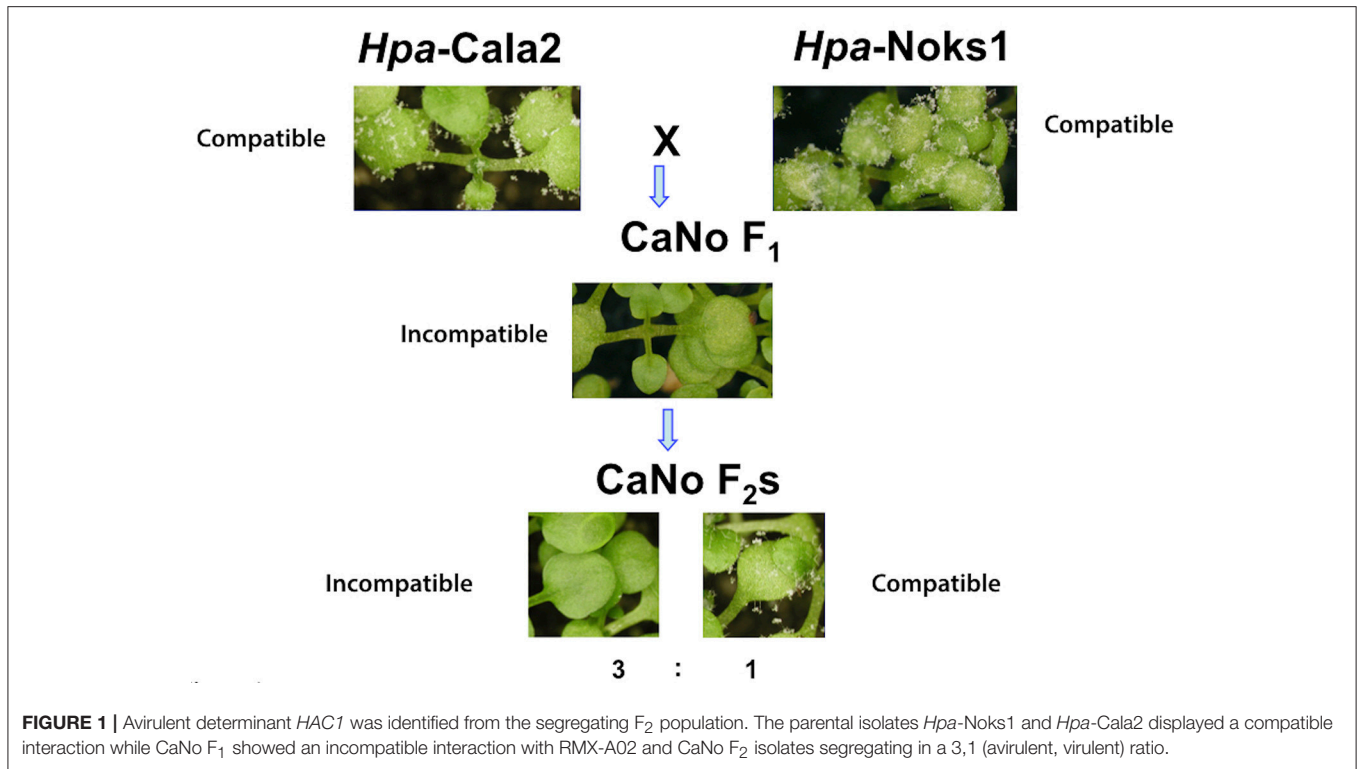
Discovering Cryptic Avirulence Determinant from Mating of Virulent *Hpa* Isolates

Two *Hpa* isolates, *Cala2* and *Noks1*, were used to screen the worldwide diversity collection of 96 *A. thaliana* accessions (Nordborg et al., 2005) for variation in downy mildew response. Twenty-one accessions from this collection were susceptible in cotyledons to both of these isolates. The susceptible accessions were then screened with an F₁ isolate (referred to hereafter as CaNo F₁) that was generated from a laboratory mating of *Hpa-Cala2* and *Hpa-Noks1* (Bailey et al., 2011). Three North American accessions (RMX-A02, RMX-A180, and Yo-0) and one Swedish accession (Bil-7) were found to be resistant in cotyledons to CaNo F₁ (**Figure 1; Supplemental Table 2**).

We used an available F₂ mapping population from this F₁ isolate for further investigations. Accessions that were susceptible to both *Hpa-Cala2* and *Hpa-Noks1* but resistant to CaNo F₁ also showed resistance to some of the F₂ isolates, indicating the presence of a possible “cryptic” avirulence locus in *Hpa*. Using the *A. thaliana* accession RMX-A02, a total of 54 randomly selected CaNo F₂ isolates were screened to determine the inheritance of the avirulence determinant. A single dominant avirulence determinant could explain the phenotypic variation that segregated in the CaNo F₂ population (avirulence, virulence ratio was 43,11, with chi-square = 0.717 and *P* = 0.30, **Supplemental Table 3**). The predicted avirulence determinant was designated as *Hyaloperonospora arabidopsidis cryptic1* (*HAC1*). This result suggested the presence of a suppressor, designated *Suppressor of HAC1* (*S-HAC1*) originating from either *Hpa-Cala2* or *Hpa-Noks1* but that was not inherited by the F₁ isolate that was used to generate the F₂ population.

Fine Mapping Defines a 14 kb Interval for the *HAC1* Locus

DNA from 15 virulent and 15 avirulent F₂ isolates was pooled in equal concentrations to make up the virulent and avirulent DNA bulks, respectively, and bulk segregant mapping analysis was performed. We generated 100 bp paired-end Illumina HiSeq2500



sequencing data from the two bulked (virulent and avirulent) pools, comprising 104 million reads for the virulent bulk, and 110 million reads for the avirulent bulk. We then used the *Hpa-Noks1* genome assembly as a reference to map sequence reads from both virulent and avirulent bulks. A total of 26,722 SNP sites were then identified and examined for frequency of major alleles in the bulks. *Hpa-Noks1* contig 23137 had the highest SNP frequency (**Supplemental Table 4**). Some of these SNPs were converted to CAPS marker and were then used to map the *HAC1* locus. Once linkage was confirmed, flanking markers were used to identify the *Hpa-Emoy2* reference genome (v8.3.) Scaffold 41. A total of 190 *F₂* isolates were then screened with further markers and the *HAC1* locus was fine mapped to a 14 kb interval on the reference genome *Hpa-Emoy2*, Scaffold 41, 298,000-312,000 (**Figure 2A**).

HAC1^{Cala2} Is an RXLR-dEER Type Avirulence Determinant

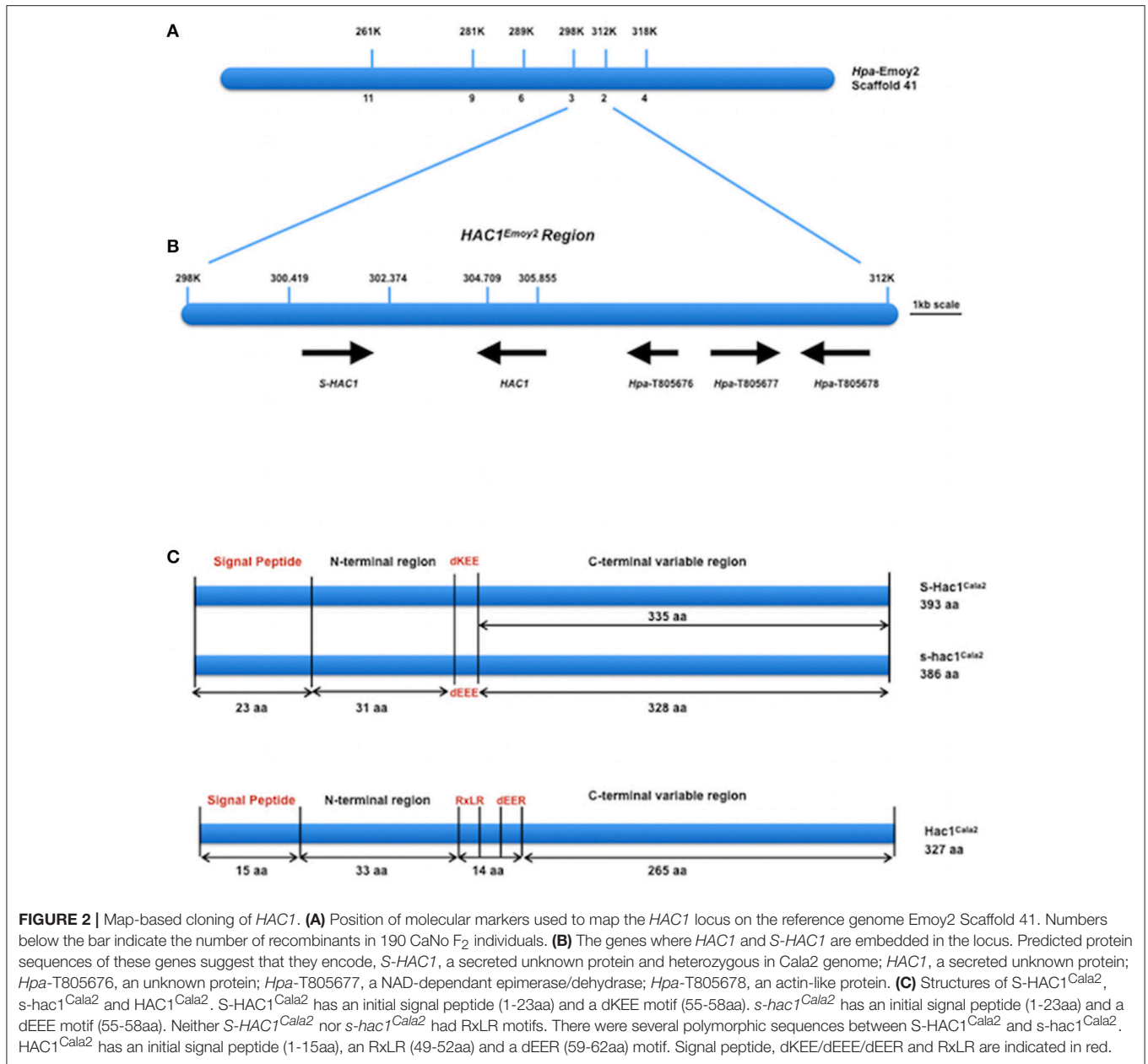
According to the EnsemblProtists annotation, this 14 kb interval in *Hpa-Emoy2* genome contains three genes without any putative effector domains and motifs, *Hpa-T805676* encoding an unknown protein, *Hpa-T805677* encoding a NAD-dependant epimerase/dehydrase (Pfam, PF01370), and *Hpa-T805678* encoding an actin-like protein (PF00022). There were also two gaps in the *Hpa-Emoy2* genome sequence assembly within the interval at position 41,300,419–302,374, and 41,304,709–305,855 (**Figure 2B**). Subsequent efforts therefore focused on PCR amplification and sequencing to fill these gaps from genomic DNA of *Hpa-Cala2*, *Hpa-Noks1*, *Hpa-Emoy2*, and a virulent and an avirulent *CaNo F₂* isolates. This revealed the

existence of a putative effector gene in each of the gaps. We then concentrated on these putative genes and a rapid isolation of cDNA ends (RACE) PCR was carried out for each. Full-length cDNAs for each gene from *Hpa-Cala2*, *Hpa-Noks1*, and *Hpa-Emoy2* were obtained and comparison to genomic DNA revealed that none of them had any intron.

In the first gap (41,300,419–302,374), two alleles of the same gene with 96% identity at the nucleotide level were identified in *Hpa-Cala2*, indicating that this gene is heterozygous. Both alleles encode a predicted protein with structural similarity to other putative effector genes; a search for domains and motifs revealed a signal peptide and a dEEE motif in one allele (designated *s-hac1^{Cala2}*, see below for details), and a signal peptide and a dKEE motif in the other (designated *S-HAC1^{Cala2}*, see below for details). This indicates that both proteins may be secreted and act as putative effectors. Neither of the alleles had the RXLR motif (**Figure 2C**). Further analysis showed *Hpa-Noks1* and *Hpa-Emoy2* were both homozygous for the *s-hac1* allele. Additionally, the *Hpa-Noks1* allele had a premature stop codon (see below for details).

In the second gap (41,304,709–305,855), a gene predicted to encode a protein with a signal peptide, an RxLR and a dEER motif was identified in *Hpa-Cala2* (**Figure 2C**) suggesting that this protein may also be secreted and act as a putative effector. No heterozygosity was detected in this gene at *Hpa-Cala2*, *Hpa-Noks1*, and *Hpa-Emoy2* genomes. Both *Hpa-Noks1* and *Hpa-Emoy2* alleles had premature stop codon.

Hpa-Noks1 and *Hpa-Cala2* are virulent whereas *CaNo F₁* is avirulent in cotyledons of the accession RMX-A02. Since sequence information of the putative effector genes in the interval



from *Hpa-Noks1* and the virulent F₂ isolates revealed that both have a premature stop codon, suggesting that both of them are non-functional. In contrast, *Hpa-Cala2* and the avirulent homozygous F₂ isolate have the full-length alleles indicating that the putative avirulence determinant may come from the parent isolate *Hpa-Cala2*.

Recognition of the *HAC1* product by the corresponding *R*-gene in RMX-A02 protein should initiate a defense response and therefore, be amenable to identify the avirulent determinant. To test this, we cloned the full-length copies of the putative effector genes (with dEEE or dKEE motif in the first gap, and with RxLR/dEER in the second gap) from *Hpa-Cala2* and *Hpa-Noks1* into vectors with a Dex-inducible promoter and then

transformed them into RMX-A02 and Col-0 plants. Transgenic T₁, T₂ and homozygous T₃ plants were selected using Basta and the insert was confirmed with PCR (**Supplemental Figure 1**). All of the Basta-selected lines were treated with dexamethasone. Only the RMX-A02 seedlings that carried the RxLR-type effector from *Hpa-Cala2* showed a chlorotic response 3 days after treatment (**Figure 3**) indicating an *R*-gene mediated cell death. Growth of these plants was stunted and in many cases individuals could not be recovered for producing seed. No altered phenotype was observed in any of the transgenic Col-0 plants indicating the defense response was race specific. Similarly, neither the *Hpa-Noks1* variant of the RxLR-type effector nor the variant of the second dEEE/dKEE type putative effectors triggered a defense

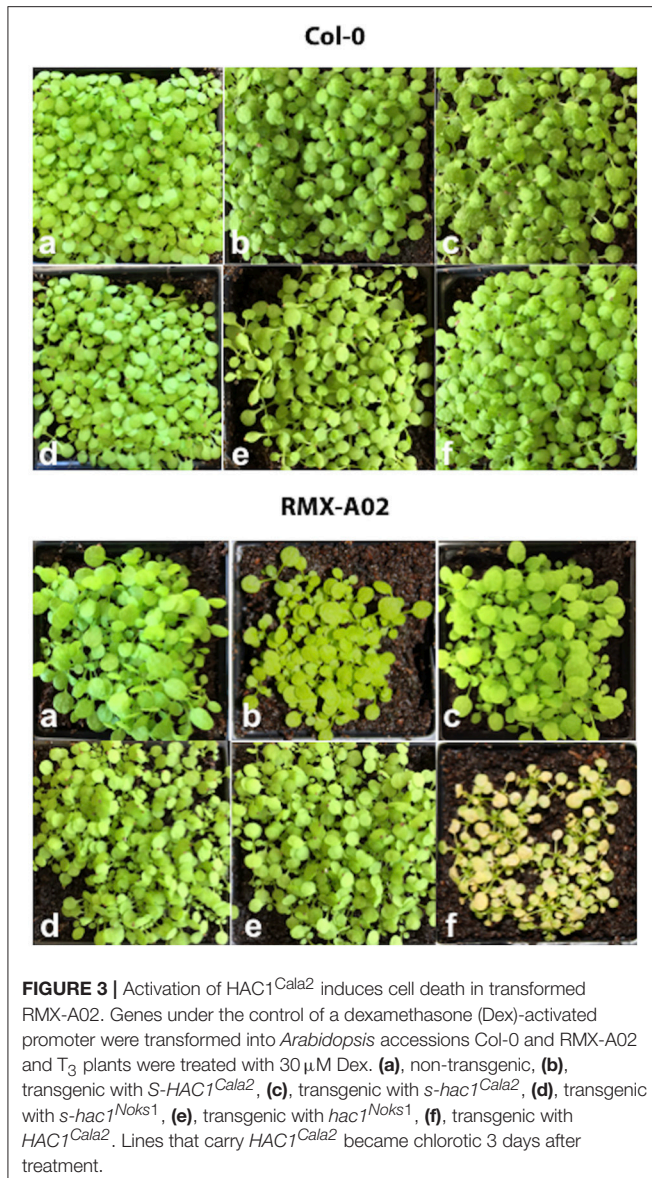


FIGURE 3 | Activation of $HAC1^{Cala2}$ induces cell death in transformed RMX-A02. Genes under the control of a dexamethasone (Dex)-activated promoter were transformed into *Arabidopsis* accessions Col-0 and RMX-A02 and T_3 plants were treated with $30 \mu\text{M}$ Dex. (a), non-transgenic, (b), transgenic with $S-HAC1^{Cala2}$, (c), transgenic with $s-hac1^{Cala2}$, (d), transgenic with $s-hac1^{Noks1}$, (e), transgenic with $hac1^{Noks1}$, (f), transgenic with $HAC1^{Cala2}$. Lines that carry $HAC1^{Cala2}$ became chlorotic 3 days after treatment.

response in RMX-A02 (Figure 3). This supports the conclusion that $HAC1$ avirulence in *A. thaliana* accession RMX-A02 is determined by recognition of the RxLR-type protein inherited from Hpa -Cala2 and this *Avr* gene is designated $HAC1^{Cala2}$.

Pathogen Genetics Supports Heterozygosity in $HAC1$ Locus in Hpa -Cala2

As described above, the gene discovered in the first gap of the genome sequence of Hpa -Cala2 is heterozygous, with alleles having either a dEEE or dKEE motif. Both virulent and avirulent CaNo F_2 isolates had only the putative effector with the dEEE motif, indicating that this allele does not influence the virulence of the pathogen on RMX-A02. This implies that the dEEE allele rather than the dKEE allele from Hpa -Cala2 was inherited during

the generation of the F_1 . Thus, the presence of the dKEE allele in Hpa -Cala2 may somehow suppress the $HAC1^{Cala2}$ -triggered defense response. If true, then cultures derived from selfed-oospores of Hpa -Cala2 should segregate for phenotypic variation of virulence/avirulence in RMX-A02. To test this, 29 selfed Hpa -Cala2 lines were screened using high-resolution melt curve (HRM) analysis. The segregation ratio obtained was 8,15,6 ratio (dKEE/dKEE, dKEE/dEEE, dEEE/dEEE; 1,2,1 ratio) confirming the segregation of alleles (Figure 4). Seven of these selfed lines were used to test interactions on RMX-A02. Five lines were virulent and two avirulent correlating well with the HRM data. These results indicate that the dKEE allele is epistatic over $HAC1^{Cala2}$ either by inducing susceptibility before $HAC1^{Cala2}$ triggers defense or by somehow interfering directly with the function of the $HAC1^{Cala2}$ effector. Since Hpa -Cala2 is virulent and heterozygous, the dKEE-containing allele is the originally predicted dominant allele, designated $S-HAC1^{Cala2}$ (*Suppressor of H. arabidopsidis cryptic 1*), whereas the allele with the dEEE motif would be the recessive or $s-hac1^{Cala2}$ allele.

Overexpression of $S-HAC1^{Cala2}$ in *Arabidopsis* Alters Interaction Phenotype

Since pathogen genetics and molecular studies suggested that $S-HAC1^{Cala2}$ plays a role in Hpa -Cala2 virulence on RMX-A02, we tested whether overexpression of this gene within the plant alters the $HAC1^{Cala2}$ -triggered defense response. The $S-HAC1^{Cala2}$ gene was cloned under a 35S promoter, transformed into RMX-A02 plants and inserts were confirmed by PCR (Supplemental Figure 2). Homozygous T_3 lines were then challenged with a representative avirulent F_2 isolate (CaNo F_2 110) and Hpa -Cala2 and Hpa -Emoy2 as virulent control isolates. In controls, transgenic lines inoculated with Hpa -Cala2 or Hpa -Emoy2 did not show any alterations in pathogen growth and the lines gave wild-type levels of susceptibility.

The typical defense response of untransformed RMX-A02 seedlings inoculated with CaNo F_2 110 was without any symptoms such as flecks, pitting, or trailing necrosis; the cotyledons remained green and very rarely sporulation was observed. RMX-A02 lines carrying the $S-HAC1^{Cala2}$ gene exhibited wild-type development of rosettes and flowering, indicating that overexpression of this gene did not have a physiological effect on the plant. However, T_3 transgenic lines challenged with avirulent CaNo F_2 110 displayed enhanced sporulation, at L3 level interaction phenotype (Tör et al., 2002). Enhanced pathogen growth was also confirmed with trypan blue staining of infected tissues (Figure 5A). High-level sporulation expected for full susceptibility was not observed, indicating the transgene did not fully suppress the avirulence conferred by $HAC1^{Cala2}$ when expressed *in planta*. *Ws-eds1*, *Ler-0*, and Col-0 inoculated with CaNo F_2 110 displayed full sporulation as expected (Figure 5A).

The biomass of CaNo F_2 110 within the transgenic and non-transgenic lines was also quantified using qPCR. A significant increase in pathogen biomass was detected within the RMX-A02 lines carrying the $S-HAC1^{Cala2}$ gene lines (Figure 5B) indicating the presence of the $S-HAC1^{Cala2}$ gene contributes to pathogen growth.

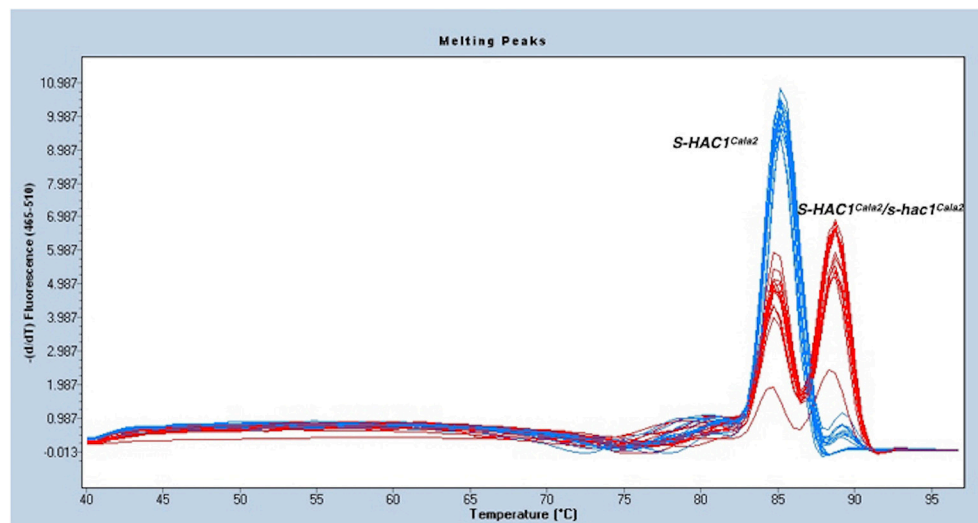


FIGURE 4 | *S-HAC1^{Cala2}* and *s-hac1^{Cala2}* alleles segregate in selfed *Hpa-Cala2*. Twenty-nine cultures derived from oospores of selfed *Hpa-Cala2* were subjected to high-resolution melt curve analysis using *S-HAC1^{Cala2}*-specific primers. Blue peaks show homozygous *S-HAC1^{Cala2}* lines and red peaks show heterozygous lines. The experiment has been repeated with the *s-hac1^{Cala2}* specific primers and the same results were obtained.

Sequence and Expression Analysis of *HAC1^{Cala2}*, *S-HAC1^{Cala2}* and *s-hac1^{Cala2}*

The open reading frame of the *HAC1^{Cala2}* gene encodes a predicted protein of 327 amino acids (molecular mass of 37.262 kDa). Domain and motif searches of the *HAC1^{Cala2}* protein identified a signal peptide (M1-A15), an RxLR (49 to 52 aa) and dEER (59-62 aa) motifs (Figure 6A). Transmembrane prediction using the TMHMM server (Krogh et al., 2001) did not identify any TM domain, suggesting that *HAC1^{Cala2}* is a soluble protein. Analysis of *HAC1^{Noks1}* and *HAC1^{Emoy2}* sequences indicated that these proteins are identical at the N-terminal, but both of them lack the RxLR motif and both have a premature stop codon around the dEER (58 aa) motif (Figure 6A). This stop codon has originated from indels at the nucleotide level that cause a frame shift (Supplemental Figure 3). BLAST searches against the *Hpa-Emoy2* database (<http://eumicrobedb.org>) did not reveal a significant alignment of *HAC1^{Cala2}* with any unigene. Using *HAC1^{Cala2}*, the TBLASTN search against Ensembl EST database revealed 66% identity to *HpaT801867* (*ATR1^{NDWSB}* allele) and 48% identity to *HpaT813746*, two avirulence protein-like proteins. Analysis of structure of the *HAC1^{Cala2}* protein using Phyre2 (Kelley et al., 2015) revealed that 55% of the total amino acid sequences can be modeled onto the *ATR1* effector protein from *Hpa*, supporting the hypothesis that the *HAC1^{Cala2}* protein may act as an effector protein (Supplemental Figure 4).

The open reading frame of the *S-HAC1^{Cala2}* allele encodes a predicted protein of 393 aa (molecular mass of 43.225 kDa). Domain and motif searches on the *S-HAC1^{Cala2}* protein identified a signal peptide (M1-T23), and a dKEE (55-58 aa) motif (Figure 6B), and no TM domain has been identified. *s-hac1^{Cala2}* has similar motifs but has the dEEE instead of dKEE (Figure 6B). *S-HAC1^{Cala2}* and *s-hac1^{Cala2}* share 94.9% identity. *s-hac^{Noks1}* has a premature stop codon (94 aa) and

analysis of *S-HAC1^{Cala2}*, *s-hac1^{Cala2}*, *s-hac^{Noks1}*, and *s-hac^{Emoy2}* sequences revealed that the N-termini of these proteins are conserved (Figure 6B). Alignment of nucleotide sequences of *S-HAC1^{Cala2}*, *s-hac1^{Cala2}*, *s-hac^{Noks1}*, and *s-hac^{Emoy2}* indicate the level of polymorphism (Supplemental Figure 5). BLAST and TBLASTN searches with *S-HAC1^{Cala2}*, *s-hac1^{Cala2}* against Ensembl did not reveal any significant alignment. In addition, structure analysis of *S-HAC1^{Cala2}* and *s-hac1^{Cala2}* using Phyre2 did not detect any (remote) homologs for the protein.

Expression of *HAC1^{Cala2}* and *S-HAC1^{Cala2}* in *Hpa-Cala2* was investigated over a time course. Total RNA was isolated from uninfected (control) or infected tissues at 1–7 days post inoculation (dpi). Gene specific primers were used for reverse transcriptase mediated (RT) PCR analysis (Supplemental Figure 6). Expression of both genes was detected in infected tissues at 2 dpi. To obtain further insight into the expression level of these genes, quantitative PCR was carried out with total RNA isolated from *Arabidopsis* seedlings infected *Hpa-Cala2* at 3, 4, and 7 dpi using gene specific primers for *HAC1^{Cala2}*, *S-HAC1^{Cala2}* and *s-hac1^{Cala2}*. All three genes showed increasing levels of expression over a week, and the expression levels of *HAC1^{Cala2}* and *S-HAC1^{Cala2}* were very similar. The expression level of *s-hac1^{Cala2}* was significantly lower than that of *HAC1^{Cala2}* and *S-HAC1^{Cala2}* (Figure 7).

Other Heterozygous Suppressor Genes Exists in *Hpa-Cala2*

To investigate whether any other heterozygous alleles might exist, we used the parent isolate *Hpa-Cala2* and two progeny lines from selfed *Hpa-Cala2*, *Hpa-Cala2S2*, and *Hpa-Cala2S5*, to screen 50 of the 96 worldwide diversity collection of

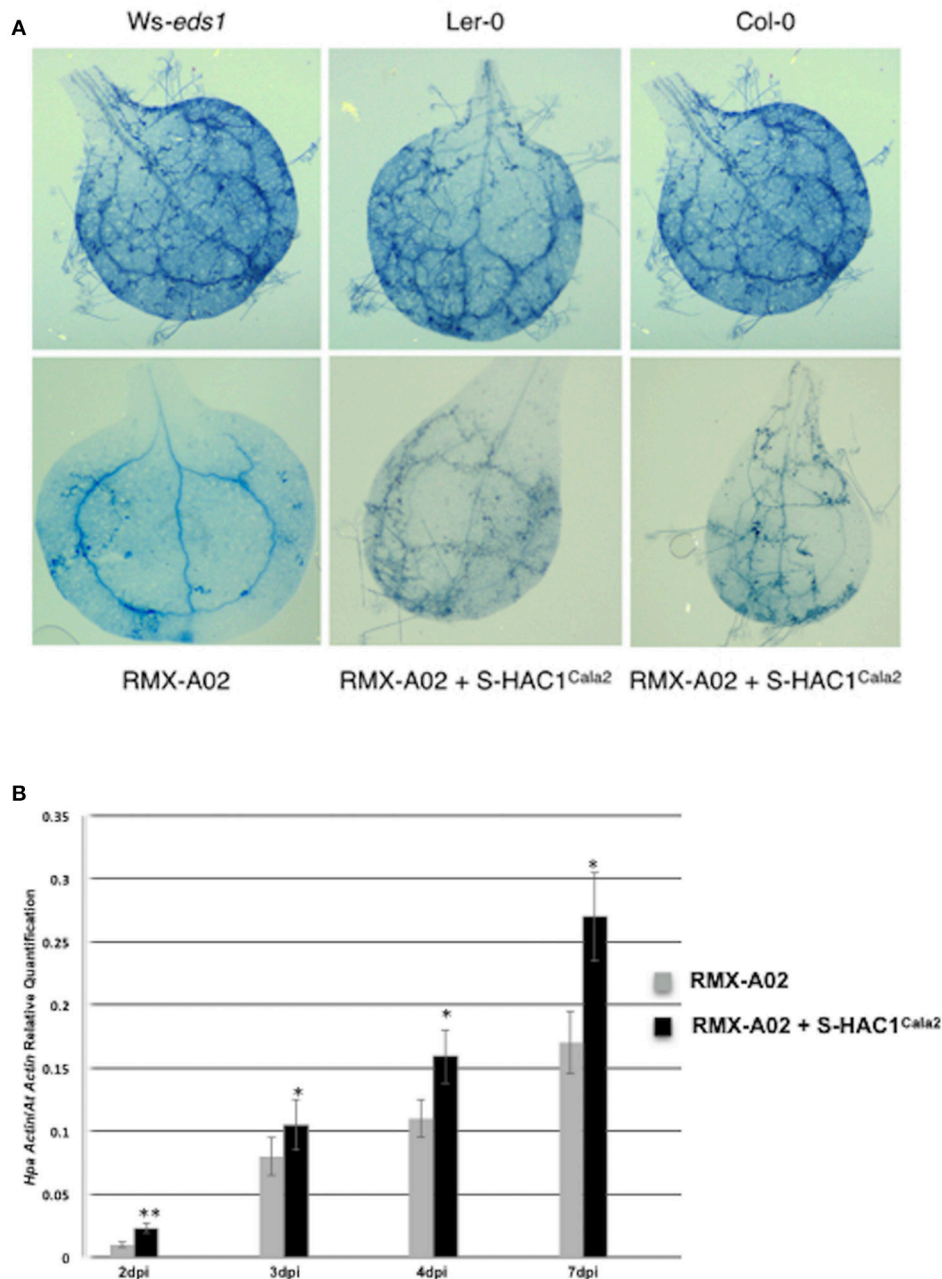


FIGURE 5 | Overexpression of *S-HAC1^{Cala2}* in RMX-A02 displays altered phenotype and biomass production. The *S-HAC1^{Cala2}* gene was cloned under a 35S promoter and introduced to RMX-A02 plants. Homozygous T₃ lines were challenged with avirulent F₂ isolate, CaNo F₂ 110. **(A)**, wild-type and transgenic seedlings inoculated with CaNo F₂ 110 and stained with trypan blue 7 days post inoculation (dpi); **(B)**, pathogen biomass production in transgenic and non-transgenic RMX-A02. Relative abundance of *Hpa-Actin* (*Hpa-807716*) to *Arabidopsis At5g46630* gene was calculated from infected plant materials 2, 3, 4, and 7 dpi. Three samples were included for each analysis and the experiments were repeated three times. The increase in pathogen biomass in RMX-A02+S-HAC1^{Cala2} compared with that in the RMX-A02 control was statistically significant (**P* < 0.05, ***P* < 0.01; Student's *t*-test).

A. thaliana accessions (Nordborg et al., 2005). Interestingly, the isolates displayed different interaction phenotypes with these accessions (**Supplemental Table 5**), indicating the parent

isolate was heterozygous at other loci. Forty accessions gave the same reaction to *Hpa-Cala2*, *Hpa-Cala2S2*, and *Hpa-Cala2S5*. However, 10 of the accessions differed in their responses,

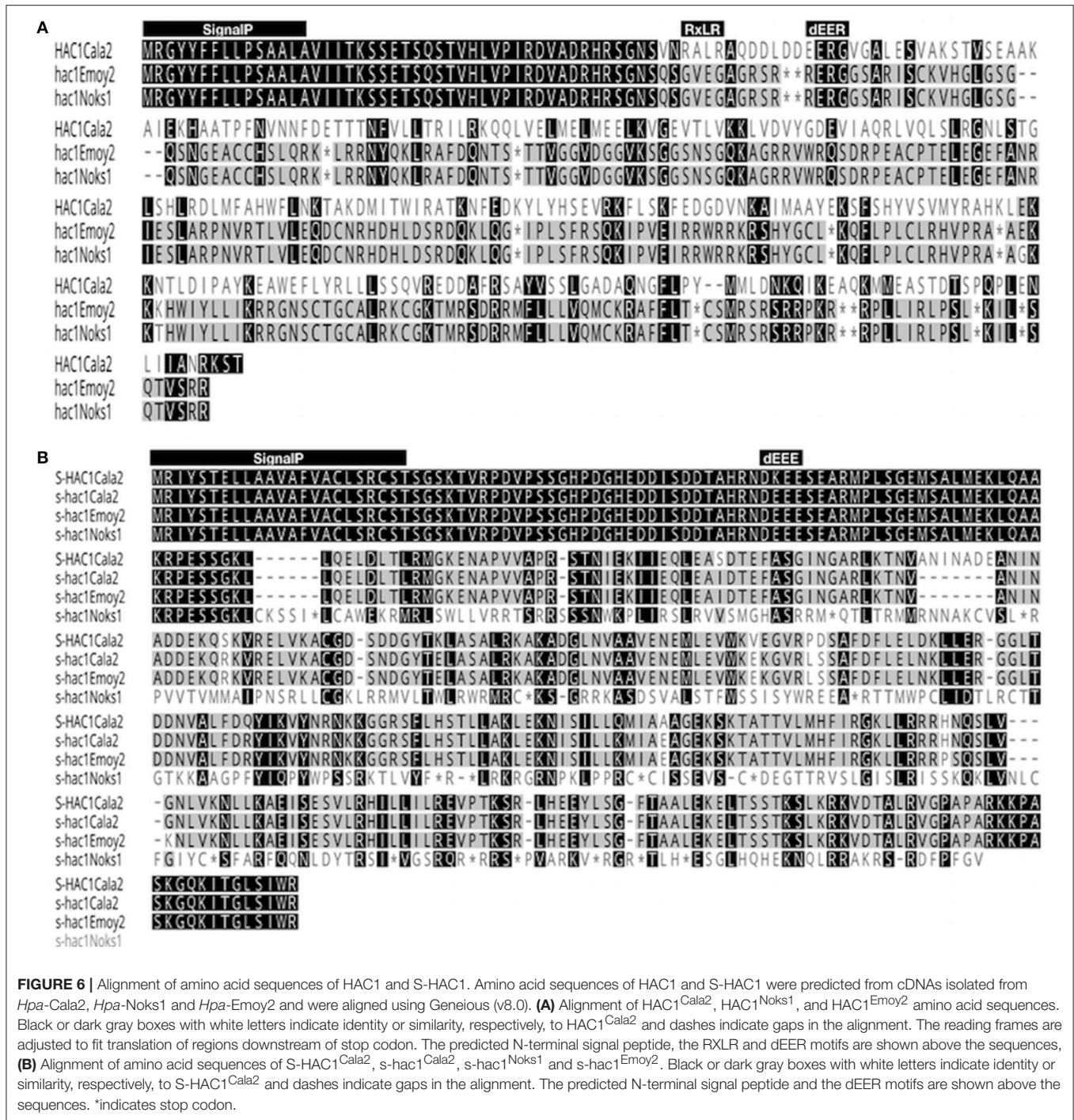


FIGURE 6 | Alignment of amino acid sequences of HAC1 and S-HAC1. Amino acid sequences of HAC1 and S-HAC1 were predicted from cDNAs isolated from *Hpa-Cala2*, *Hpa-Noks1* and *Hpa-Emoy2* and were aligned using Geneious (v8.0). **(A)** Alignment of HAC1^{Cala2}, HAC1^{Noks1}, and HAC1^{Emoy2} amino acid sequences. Black or dark gray boxes with white letters indicate identity or similarity, respectively, to HAC1^{Cala2} and dashes indicate gaps in the alignment. The reading frames are adjusted to fit translation of regions downstream of stop codon. The predicted N-terminal signal peptide, the RXLR and dEER motifs are shown above the sequences, **(B)** Alignment of amino acid sequences of S-HAC1^{Cala2}, s-hac1^{Cala2}, s-hac1^{Noks1} and s-hac1^{Emoy2}. Black or dark gray boxes with white letters indicate identity or similarity, respectively, to S-HAC1^{Cala2} and dashes indicate gaps in the alignment. The predicted N-terminal signal peptide and the dEER motifs are shown above the sequences. *indicates stop codon.

including eight (Bil-7, Tamm-2, Rmx-A02, Eden-2, Mz-0, Kz-1, Rmx-A180, Ra-0) that were susceptible to the parent isolate *Hpa-Cala2*. Only four of these accessions (Mz-0, Kz-1, Sq-8, Ws-0) were susceptible to *Hpa-Cala2S2*, and only six (Bil-7, Tamm-2, Rmx-A02, Eden-2, Rmx-A180, Ra-0) were susceptible to *Hpa-Cala2S5* (Table 1). These findings suggest that heterozygosity may exist and be maintained in other loci of the *Hpa-Cala2* genome.

DISCUSSION

Cryptic avirulence is a phenomenon that was first described by H.H. Flor during his seminal research on interactions between flax and the basidiomycete fungus *M. lini* (Flor, 1946) and this phenomenon has subsequently been confirmed in fungal genetic experiments by other researchers (Lawrence et al., 1981; Ellingboe, 1992; Lau et al., 1993). Here we

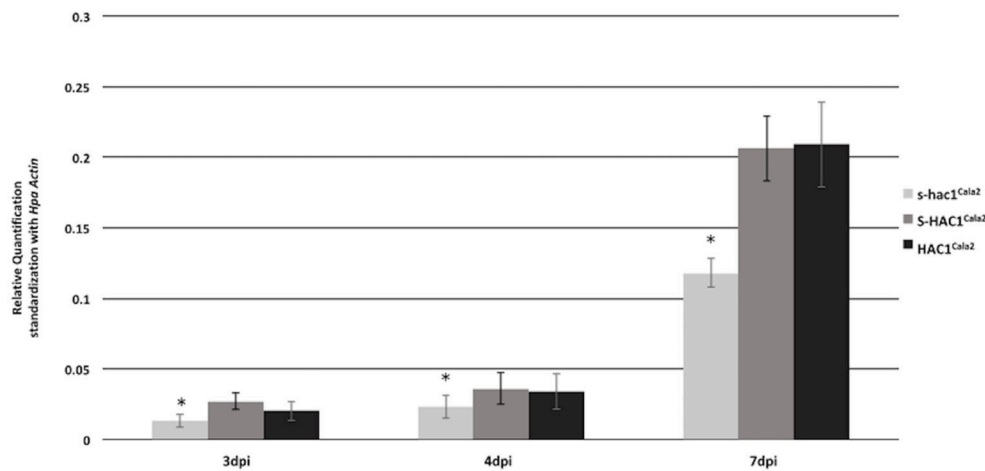


FIGURE 7 | Expression analysis of *s-hac1^{Cala2}*, *S-HAC1^{Cala2}* and *HAC1^{Cala2}*. Total RNA was isolated from infected *Hpa-Cala2* at 3, 4 and 7dpi. Quantitative Real-time PCR was carried out using gene specific primers for *HAC1^{Cala2}*, *S-HAC1^{Cala2}* and *s-hac1^{Cala2}*. Fifteen seedlings from each genotype made up a sample and three replicates were used for each sample, the experiments were repeated three times with similar results. Expression level of *s-hac1^{Cala2}* was significantly lower than that of *S-HAC1^{Cala2}* and *HAC1^{Cala2}* in *Hpa-Cala2* background. Asterisks denote statistical significance in two-tailed Student's *t*-test ($p < 0.05$).

TABLE 1 | Interaction phenotypes of *Arabidopsis* accessions with the parent isolate *Hpa-Cala2* and two offspring.

Accessions	<i>Hpa-Cala2</i>	<i>Hpa-Cala2S2*</i>	<i>Hpa-Cala2S5*</i>
Bil-7	S	R	S
Tamm-2	S	R	S
Rmx-A02	S	R	S
Eden-2	S	R	S
Mz-0	S	S	R
Kz-1	S	S	R
Rmx-A180	S	R	S
Sq-8	R	S	R
Ra-0	S	R	S
Ws-0	R	S	R

S, Susceptible; R, Resistance; **Hpa-Cala2S2* and *Hpa-Cala2S5* are derived from oospores generated from *Hpa-Cala2*.

present pathology, genetic and molecular evidence that this phenomenon also occurs in a biotrophic oomycete. Using the *Arabidopsis-Hyaloperonospora* experimental model, we showed that the *Arabidopsis* accession RMX-A02 is susceptible to two standard isolates (*Hpa-Cala2* and *Hpa-Noks1*) but resistant to an F₁ derived from these isolates (CaNo F₁) and that a single corresponding avirulence locus is indicated by segregation in F₂ progeny derived from this F₁. This was confirmed using fine-mapping and genomic sequencing to clone an avirulence determinant (designated *HAC1^{Cala2}*) and a heterozygous avirulence suppressor gene in the same map interval (designated *S-HAC1^{Cala2}/s-hac1^{Cala2}*). Both genes encode putative effector proteins.

In most cases, a map-based gene cloning strategy uses parental lines that differ in contrasting phenotypes (e.g., resistant vs. susceptible plants; or avirulent vs. virulent pathogen isolates)

to generate a mapping population. However, the parent isolates used in the present study (*Hpa-Cala2* and *Hpa-Noks1*) were both virulent on the same *Arabidopsis* accession, RMX-A02. Thus, we could not know from which parent the hidden or cryptic avirulence allele originated. Cryptic alleles are phenotypically silent DNA sequences and have been reported in prokaryotic microorganisms as well as in fungi (Hall et al., 1983; Le Gac et al., 2007). Several molecular explanations have been postulated including, (1) spontaneous occurrence by mutation or rearrangements, (2) action of a second suppressor locus, and (3) epigenetic control. They may however be activated in a few individuals of a large population by mutation, recombination, insertion elements or by other genetic mechanisms (Hall et al., 1983; Li, 1984).

In the present investigation, we used next generation sequencing to reveal the loci involved. Virulent and avirulent bulks were sequenced, as well as the genomes of the parental isolates, and we used the polymorphic nature of the isolates to screen 26722 SNP sites, enabling us to identify a contig from *Hpa-Noks1* genome linked to the locus. The *HAC1* locus was mapped to a 14 kb interval using an experimental population of 190 F₂ isolates, and haplotype sequence information from *Hpa-Cala2*, *Hpa-Noks1*, and *Hpa-Emoy2* to characterize the high degree of polymorphism in the interval.

All of the *R/AVR* gene pairs that have previously been cloned from the *Hpa-Arabidopsis* system, including *RPP1/ATR1* (Botella et al., 1998; Rehmany et al., 2005) and *RPP13/ATR13* (Bittner-Eddy et al., 1999; Allen et al., 2004), have fallen into the NLR type of *R*-genes and RxLR-dEER class of effectors. *HAC1^{Cala2}* has the canonical signal and translocation peptides, RxLR-dEER, and triggers a defense response in RMX-A02. Previously, we used the CaNo F₂ 110 to investigate the corresponding gene in RMX-A02 and mapped the locus in the *Arabidopsis* genome to chromosome 4 within an interval of 35 kb containing

three *R*-genes in the *RPP4/RPP5* locus (unpublished data). Thus, *HAC1^{Cala2}*-triggered defense responses in the RMX-A02 background are very highly likely to be mediated by an NLR type *R*-gene.

A large number of RxLR or RxLR-like effectors have been identified in various downy mildew pathogens and *Phytophthora* species (Bailey et al., 2011; Anderson et al., 2015) and molecular studies on several of these effectors have shown that they suppress plant immunity (Sohn et al., 2007). It was interesting that the structure of *HAC1^{Cala2}* could be modeled with high confidence onto the ATR1 effector protein. To investigate the RPP1/ATR1 interaction, Chou et al. (2011) determined the crystal structure of ATR1 and identified the critical recognition sites of the effector protein. They concluded that oomycete effectors that share the same lineage as ATR1 rapidly evolve to escape host detection. In this case, if *HAC1^{Cala2}* is indeed from the same family as ATR1, it can be proposed that *HAC1^{Cala2}* alleles, *hac1^{Noks1}*, and *hac1^{Emoy2}*, have already evolved to avoid recognition as they have premature stop codons, enabling *Hpa-Noks1* and *Hpa-Emoy2* to be virulent on RMX-A02.

A diploid organism can be heterozygous at a gene locus when its cells contain two different alleles of a gene and use this for its own advantage. The importance of heterozygosity for virulence in fungi and oomycetes has been recognized for a while and in some cases documented. For example, a high level of heterozygosity for virulence in two populations of *Puccinia recondita* (wheat leaf rust fungus) has been found (Kolmer, 1992). Similarly, genomic sequences of *P. striiformis* f. sp. *tritici* (*Pst*-

wheat stripe rust fungus) revealed the presence of heterozygosity (Zheng et al., 2013). Population studies on *M. grisea* (rice blast fungus) using PCR markers identified six of the loci investigated to be heterozygous (Babu et al., 2013). Genomic investigations on *Phytophthora capsici* revealed the loss of heterozygosity, which has been proposed to be a rapid mechanism for fixing alleles and may be an important component of adaptability (Lamour et al., 2012). Similarly, screening of 652 *P. infestans* isolates from commercial potato fields in the Netherlands during a ten-year period using 12 informative microsatellite markers and mitochondrial haplotypes detected a low level of heterozygosity (Li et al., 2012). It has been reasoned that a pathogen could gain a selective advantage from a heterozygous genotype by increasing the pathogen's ability to adapt to a changing host environment such as overcoming the host's resistance mechanism (Zheng et al., 2013).

In the current investigation, it is interesting that heterozygosity of a putative effector gene was revealed in one isolate *Hpa-Cala2* but not in two other standard isolates (*Hpa-Noks1* and *Hpa-Emoy2*) (Figure 8). Heterozygote genotypes are known to have a higher relative fitness than either the homozygote dominant or homozygote recessive genotypes, known as heterozygous advantage (Hedrick, 2012). There are many examples of heterozygous advantage in living systems. For example, the Major Histocompatibility Complex (MHC) loci are highly polymorphic heterozygous loci that control immunological recognition of pathogens in animals and confer a selective advantage by enhancing resistance to infectious diseases

Suppressor allele		Avr allele		Pathogen	Isolate
<i>S-HAC1^{Cala2}</i>	<i>s-hac1^{Cala2}</i>	<i>HAC1^{Cala2}</i>	<i>HAC1^{Cala2}</i>	V	<i>Hpa-Cala2</i>
<i>s-hac1^{Noks1}</i>	<i>s-hac1^{Noks1}</i>	<i>hac1^{Noks1}</i>	<i>hac1^{Noks1}</i>	V	<i>Hpa-Noks1</i>
<i>s-hac1^{Cala2}</i>	<i>s-hac1^{Noks1}</i>	<i>HAC1^{Cala2}</i>	<i>hac1^{Noks1}</i>	A	CaNo-F ₁
<i>s-hac1^{Emoy2}</i>	<i>s-hac1^{Emoy2}</i>	<i>hac1^{Emoy2}</i>	<i>hac1^{Emoy2}</i>	V	<i>Hpa-Emoy2</i>

FIGURE 8 | Genotypes of three *Hpa* isolates at the *HAC1* locus. Sequencing and pathology results were used to determine the genotypes of isolates. In *Hpa-Cala2*, virulence on RMX-A02 results from the combination of an active suppressor (*S-HAC1^{Cala2}*) and an active avirulence (*HAC1^{Cala2}*) allele. In the presence of an inactive suppressor (*s-hac1^{Cala2}*) and an active avirulence (*HAC1^{Cala2}*) allele, the interaction results in avirulence. In *Hpa-Noks1* and *Hpa-Emoy2*, the putative avirulence gene is inactive due to mutations, thus both are virulent on RMX-A02.

(Penn et al., 2002). A well-established case of heterozygous advantage in humans is that of the genes involved in sickle cell anemia (Luzzatto, 2012) and Cystic Fibrosis (Modiano et al., 2007). In plant breeding programmes, hybrid vigor generated from crosses between inbred lines from different genetic backgrounds, is an example of heterozygous advantage used routinely for higher crop yield (Whitford et al., 2013). However, the majority of studies on heterozygosity in fungi and oomycete pathogens have been within the field of population genetics and there has been no investigation of heterozygosity at the level of individual locus or effector genes. Segregation of a suppressor/effector after sexual reproduction (as observed in this study) means that a proportion of the progeny will have an active Avr effector, whereas others will not. This may be advantageous to the pathogen by increasing the pathogen's ability to adapt to a changing host environment.

A secreted effector can both trigger and suppress *R* gene-based immunity. For example, *F. oxysporum* f.sp. *lycopersici* (*Fol*) effector *Avr1* triggers a defense response when the host plant, tomato, carries a matching *R*-gene (*I* or *I-1*). However, *Avr1* suppresses the protective effect of two other host *R*-genes, *I-2* and *I-3* (Houterman et al., 2008). Similarly, IPI-04, an effector protein of *P. infestans*, has been shown not only to elude detection by the host potato protein RB, but also to block recognition of the effector protein IPI-01, leading to suppression of RB-mediated host cell death (Halterman et al., 2010; Chen et al., 2012). A similar scenario may exist for the *Hpa*-Cala2 RMX-A02 interactions, where S-HAC1^{Cala2} may suppress the HAC1^{Cala2}-triggered host immunity or interfere with its function. Suppression of HAC1^{Cala2}-triggered immunity may occur within the host cell. For this to happen, S-HAC1^{Cala2} has to be delivered inside the host cell and may target the same host component as HAC1^{Cala2}. Alternatively, S-HAC1^{Cala2} may physically bind to HAC1^{Cala2} within the pathogen or inside the host cell, promoting conformational changes within HAC1^{Cala2} and preventing either the secretion of HAC1^{Cala2} from the pathogen, its entry into the host cell or the recognition of HAC1^{Cala2} by the host intracellular receptor. We hope to investigate this further with yeast two-hybrid and pull-down experiments.

Overexpression of *S-HAC1^{Cala2}* in RMX-A02 plants did not confer any resistance phenotype. However, when these transgenic lines were challenged with the avirulent CaNo F₂ 110 isolate (carrying *HAC1^{Cala2}* and *s-hac1^{Cala2}*), phenotypic alterations were observed, indicating that S-HAC1^{Cala2} may have interacted with a pathogen-delivered protein, most likely to be HAC1^{Cala2}, in the apoplast or cytoplasm of the host cell. Surprisingly, full suppression of HAC1^{Cala2}-triggered resistance was not observed in these transgenic lines carrying *S-HAC1^{Cala2}*. This may indicate that S-HAC1^{Cala2} needs to interact with HAC1^{Cala2} within the pathogen or apoplast. Alternatively, it may require posttranslational modifications (PTM) by the pathogen, such as phosphorylation, SUMOylation, methylation, ubiquitination, or acetylation (Hewezi, 2015). Nevertheless, the results of this study suggest that the combination of HAC1^{Cala2} and S-HAC1^{Cala2} may dictate the race-specificity of *Hpa*-Cala2 on the *Arabidopsis* accession RMX-A02.

Hpa is a diploid, homothallic pathogen, which means that a haploid antheridium and oogonium are produced within the same thallus to generate oospores. Frequent sexual reproduction in a homothallic pathogen would be expected to give rise to a largely homozygous genome and so maintenance of heterozygosity at the *HAC1* or other loci in *Hpa*-Cala2 may be surprising. However, this and many other experimental isolates have been originally single spored and maintained in the laboratory largely through asexual propagation. In a diploid clonal population, mutation events at each locus lead to an accumulation of heterozygosity over time (Balloux et al., 2003); thus, it would be expected that there may be considerable heterozygosity in experimental isolates where there is an absence of frequent sexual reproduction. In addition, sexual crosses between expressed and silenced *Avr* alleles can result in varying outcomes and unusual inheritance patterns for *Avr* gene expression in progeny (Na and Gijzen, 2016).

The use of selfed lines *Hpa*-Cala2S2 and *Hpa*-Cala2S5 indicated that other suppressor loci within *Hpa*-Cala2 might be heterozygous and so the question arises as to whether heterozygosity is a widespread phenomenon in *Hpa*. To investigate this, we took advantage of the fact that *Hpa* isolates have been used in different laboratories to screen the same *Arabidopsis* diversity collections and some published data are available. For example, in investigations by both Krasileva et al. (2011) and Nemri et al. (2010), interaction phenotypes of isolates *Hpa*-Emwal and *Hpa*-Emco5 (among other isolates) on the 83 *Arabidopsis* accessions were assessed. However, different results were obtained by these authors for at least 12 *Arabidopsis* accessions (**Supplemental Table 6**). This discrepancy may have arisen if each group obtained their isolates from different oospores of a segregating population, indicating the existence of heterozygosity at different loci. In addition, it should be remembered that natural populations of *Hpa* are polycyclic, reproducing many times asexually (leading to an increase in heterozygosity) as well as sexually, before overwintering as oospores; also, despite being homothallic, in mixed populations, outcrossing with other races is possible. Thus, it is very probable that natural populations of *Hpa* have considerable heterozygosity. Evidence of outcrossing in other homothallic oomycetes, such as *P. ultimum* (Francis and St. Clair, 1993) and *P. aphanidermatum* (Lee et al., 2010) has also been used to explain high levels of heterozygosity in these populations.

AUTHOR CONTRIBUTIONS

MT and AW-T: Planned and designed the research; AW-T, MT, VC, and OT: Conducted the laboratory work; AW-T, MT, and DS: Analyzed the data; MT, AW-T, EH, and DS: Interpreted the data and wrote the manuscript.

FUNDING

This work was supported by grant F-09 963/A (MT) from the Leverhulme Trust. Financial support from the Turkish Ministry of Education to OT is gratefully acknowledged.

ACKNOWLEDGMENTS

We are grateful to Yiguo Hong for critically reading the manuscript.

SUPPLEMENTARY MATERIAL

The Supplementary Material for this article can be found online at: <https://www.frontiersin.org/articles/10.3389/fpls.2018.00265/full#supplementary-material>

Supplemental Figure 1 | PCR confirmation of *HAC1^{Cala2}* inserts in transgenic RMX-A02 plants.

Supplemental Figure 2 | PCR confirmation of inserts carrying *S-HAC1^{Cala2}* gene in the transgenic RMX-A02 plants.

Supplemental Figure 3 | Alignment of nucleotide sequences of *HAC1^{Cala2}* and homologs from *Hpa-Emoy2* and *Hpa-Noks1*.

Supplemental Figure 4 | Amino acid sequences of *HAC1^{Cala2}* modeled onto the ATR1 effector 2 protein from *Hpa* using Phyr2.

Supplemental Figure 5 | Alignment of nucleotide sequences of *S-HAC1^{Cala2}* homologs from *Hpa-Cala2*, *Hpa-Emoy2*, and *Hpa-Noks1*.

Supplemental Figure 6 | Expression analysis of *HAC1^{Cala2}* and *S-HAC1^{Cala2}*.

Supplementary Table 1 | Primer sequences used in this study.

Supplementary Table 2 | Screening Nordborg/Bergelson (NB) worldwide diversity collection of 96 *Arabidopsis* accessions with *Hpa-Noks1*, *Hpa-Cala2*, CaNo F2 110 and CaNo F1.

Supplementary Table 3 | Interaction phenotypes (IP) recorded seven days after inoculation of RMX-A02 accession with CaNo F₂ isolates.

Supplementary Table 4 | Frequency of major alleles at SNP sites from different scaffolds and contigs of *Hpa-Noks1* genome.

Supplementary Table 5 | Interaction phenotypes of the parent isolate *Hpa-Cala2* and two offspring with *Arabidopsis* accessions.

Supplementary Table 6 | Comparison of interaction phenotypes obtained from two independent published studies of *Hyaloperonospora arabidopsidis* isolates *Hpa-Emwa1* and *Hpa-Emco5* on 83 *Arabidopsis* accessions of the Nordborg/Bergelson collection.

REFERENCES

- Allen, R. L., Bittner-Eddy, P. D., Grenville-Briggs, L. J., Meitz, J. C., Rehmany, A. P., Rose, L. E., et al. (2004). Host-parasite coevolutionary conflict between *Arabidopsis* and downy mildew. *Science* 306, 1957–1960. doi: 10.1126/science.1104022
- Anderson, R. G., Deb, D., Fedkenheuer, K., and McDowell, J. M. (2015). Recent progress in RXLR effector research. *Mol. Plant Microbe Interact.* 28, 1063–1072. doi: 10.1094/MPMI-01-15-0022-CR
- Babu, T. K., Sharma, R., Upadhyaya, H. D., Reddy, P. N., Deshpande, S. P., Senthilvel, S., et al. (2013). Evaluation of genetic diversity in *Magnaporthe grisea* populations adapted to finger millet using simple sequence repeats (SSRs) markers. *Physiol. Mol. Plant Pathol.* 84, 10–18. doi: 10.1016/j.pmpp.2013.06.001
- Bailey, K., Cevik, V., Holton, N., Byrne-Richardson, J., Sohn, K. H., Coates, M., et al. (2011). Molecular cloning of ATR5 Emoy2 from *Hyaloperonospora arabidopsidis*, an avirulence determinant that triggers RPP5-mediated defense in *Arabidopsis*. *Mol. Plant Microbe Interact.* 24, 827–838. doi: 10.1094/MPMI-12-10-0278
- Balloux, F., Lehmann, L., and de Meeuß, T. (2003). The population genetics of clonal and partially clonal diploids. *Genetics* 164, 1635–1644.
- Baxter, L., Tripathy, S., Ishaque, N., Boot, N., Cabral, A., Kemen, E., et al. (2010). Signatures of adaptation to obligate biotrophy in the *Hyaloperonospora arabidopsidis* genome. *Science* 330, 1549–1551. doi: 10.1126/science.1195203
- Bittner-Eddy, P., Can, C., Gunn, N., Pinel, M., Tör, M., Crute, I., et al. (1999). Genetic and physical mapping of the RPP13 locus in *Arabidopsis* responsible for specific recognition of several *Peronospora parasitica* (downy mildew) isolates. *Mol. Plant Microbe Interact.* 12, 792–802. doi: 10.1094/MPMI.1999.12.9.792
- Botella, M. A., Parker, J. E., Frost, L. N., Bittner-Eddy, P. D., Beynon, J. L., Daniels, M. J., et al. (1998). Three genes of the *Arabidopsis* RPP1 complex resistance locus recognize distinct *Peronospora parasitica* avirulence determinants. *Plant Cell* 10, 1847–1860. doi: 10.1105/tpc.10.11.1847
- Bourras, S., McNally, K. E., Müller, M. C., Wicker, T., and Keller, B. (2016). Avirulence genes in cereal powdery mildews, the gene-for-gene hypothesis 2.0. *Front. Plant Sci.* 7:241. doi: 10.3389/fpls.2016.00241
- Chen, Y., Liu, Z., and Halterman, D. A. (2012). Molecular determinants of resistance activation and suppression by *Phytophthora infestans* effector IPI-0. *PLoS Pathog.* 8:e1002595. doi: 10.1371/annotation/75775518-f06e-4148-a639-31cfc6972b2e
- Chou, S., Krasileva, K. V., Holton, J. M., Steinbrenner, A. D., Alber, T., and Staskawicz, B. J. (2011). *Hyaloperonospora arabidopsidis* ATR1 effector is a repeat protein with distributed recognition surfaces. *Proc. Natl. Acad. Sci. U.S.A.* 108, 13323–13328. doi: 10.1073/pnas.1109791108
- Clough, S. J., and Bent, A. F. (1998). Floral dip, a simplified method for *Agrobacterium*-mediated transformation of *Arabidopsis thaliana*. *Plant J.* 16, 735–743. doi: 10.1046/j.1365-313x.1998.00343.x
- Dodds, P. N., and Rathjen, J. P. (2010). Plant immunity, towards an integrated view of plant–pathogen interactions. *Nat. Rev. Genet.* 11, 539–548. doi: 10.1038/nrg2812
- Doehlemann, G., and Hemetsberger, C. (2013). Apoplastic immunity and its suppression by filamentous plant pathogens. *New Phytol.* 198, 1001–1016. doi: 10.1111/nph.12277
- Doyle, J. J. (1987). A rapid DNA isolation procedure for small quantities of fresh leaf tissue. *Phytochem. Bull.* 19, 11–15.
- Earley, K. W., Haag, J. R., Pontes, O., Opper, K., Juehne, T., Song, K., et al. (2006). Gateway-compatible vectors for plant functional genomics and proteomics. *Plant J.* 45, 616–629. doi: 10.1111/j.1365-313X.2005.02617.x
- Ellingboe, A. H. (1992). Segregation of avirulence/virulence on three rice cultivars in 16 crosses of *Magnaporthe grisea*. *Phytopathology* 82, 597–601. doi: 10.1094/Phyto-82-597
- Eulgem, T., Tsuchiya, T., Wang, X. J., Beasley, B., Cuzick, A., Tör, M., et al. (2007). EDM2 is required for RPP7-dependent disease resistance in *Arabidopsis* and affects RPP7 transcript levels. *Plant J.* 49, 829–839. doi: 10.1111/j.1365-313X.2006.02999.x
- Flor, H. H. (1946). Genetics of pathogenicity in *Melampsora lini*. *J. Agric. Res.* 73, 335–357.
- Francis, D. M., and St. Clair, D. A. (1993). Outcrossing in the homothallic oomycete *Pythium ultimum* detected with molecular markers. *Curr. Genet.* 24, 100–106. doi: 10.1007/BF00324672
- Göker, M., Riethmüller, A., Voglmayr, H., Weiss, M., and Oberwinkler, F. (2004). Phylogeny of *Hyaloperonospora* based on nuclear ribosomal internal transcribed spacer sequences. *Mycol. Prog.* 3, 83–94. doi: 10.1007/s11557-006-0079-7
- Goritschnig, S., Krasileva, K. V., Dahlbeck, D., and Staskawicz, B. J. (2012). Computational prediction and molecular characterization of an oomycete effector and the cognate *Arabidopsis* resistance gene. *PLoS Genet.* 8:e1002502. doi: 10.1371/journal.pgen.1002502
- Hall, B. G., Yokoyama, S., and Calhoun, D. H. (1983). Role of cryptic genes in microbial evolution. *Mol. Biol. Evol.* 1, 109–124.
- Halterman, D., Chen, Y., Soepe, J., Berduo-Sandoval, J., and Sanchez-Pérez, A. (2010). Competition between *Phytophthora infestans* leads to increase aggressiveness containing broad spectrum late-blight resistance. *PLoS ONE* 5:e10536. doi: 10.1371/journal.pone.0010536
- Hedrick, P. W. (2012). What is the evidence for heterozygote advantage selection? *Trends Ecol. Evol.* 27, 698–704. doi: 10.1016/j.tree.2012.08.012

- Hewezi, T. (2015). Cellular signaling pathways and posttranslational modifications mediated by nematode effector proteins. *Plant Physiol.* 169, 1018–1026. doi: 10.1104/pp.15.00923
- Holub, E. B. (2006). Evolution of parasitic symbiosis between plants and filamentous microorganisms. *Curr. Opin. Plant Biol.* 9, 397–405. doi: 10.1016/j.pbi.2006.05.011
- Holub, E. B., Beynon, J. L., and Crute, I. R. (1994). Phenotypic and genotypic characterization of interactions between isolates of *Peronospora parasitica* and accessions of *Arabidopsis thaliana*. *Mol. Plant Microbe Interact.* 7, 223–239. doi: 10.1094/MPMI-7-0223
- Houterman, P. M., Cornelissen, B. J., and Rep, M. (2008). Suppression of plant resistance gene-based immunity by a fungal effector. *PLoS Pathog.* 4:e1000061. doi: 10.1371/journal.ppat.1000061
- Jones, J. D., and Dangl, J. L. (2006). The plant immune system. *Nature* 444, 323–329. doi: 10.1038/nature05286
- Kamoun, S. (2006). A catalogue of the effector secretome of plant pathogenic oomycetes. *Annu. Rev. Phytopathol.* 44, 41–60. doi: 10.1146/annurev.phyto.44.070505.143436
- Kamoun, S., Furzer, O., Jones, J. D., Judelson, H. S., Ali, G. S., Dalio, R. J., et al. (2015). The Top 10 oomycete pathogens in molecular plant pathology. *Mol. Plant Pathol.* 16, 413–434. doi: 10.1111/mpp.12190
- Kearse, M., Moir, R., Wilson, A., Stones-Havas, S., Cheung, M., Sturrock, S., et al. (2012). Geneious Basic, an integrated and extendable desktop software platform for the organization and analysis of sequence data. *Bioinformatics* 28, 1647–1649. doi: 10.1093/bioinformatics/bts199
- Keeling, P. J., Burger, G., Durnford, D. G., Lang, B. F., Lee, R. W., Pearlman, R. E., et al. (2005). The tree of eukaryotes. *Trends Ecol. Evol.* 20, 670–676. doi: 10.1016/j.tree.2005.09.005
- Kelley, L. A., Mezulis, S., Yates, C. M., Wass, M. N., and Sternberg, M. J. (2015). The Phyre2 web portal for protein modeling, prediction and analysis. *Nat. Protoc.* 10, 845–858. doi: 10.1038/nprot.2015.053
- Koch, E., and Slusarenko, A. (1990). Arabidopsis is susceptible to infection by a downy mildew fungus. *Plant Cell* 2, 437–445. doi: 10.1105/tpc.2.5.437
- Kolmer, J. A. (1992). Virulence heterozygosity and gametic phase disequilibria in two populations of *Puccinia recondita* (wheat leaf rust fungus). *Heredity* 68, 505–513. doi: 10.1038/hdy.1992.73
- Kong, Y. (2011). Btrim, a fast, lightweight adapter and quality trimming program for next-generation sequencing technologies. *Genomics* 98, 152–153. doi: 10.1016/j.ygeno.2011.05.009
- Krasileva, K. V., Zheng, C., Leonelli, L., Goritschnig, S., Dahlbeck, D., and Staskawicz, B. J. (2011). Global analysis of Arabidopsis/Downy mildew interactions reveals prevalence of incomplete resistance and rapid evolution of pathogen recognition. *PLoS ONE* 6:e28765. doi: 10.1371/journal.pone.0028765
- Krogh, A., Larsson, B., von Heijne, G., and Sonnhammer, E. L. (2001). Predicting transmembrane protein topology with a hidden Markov model, application to complete genomes. *J. Mol. Biol.* 305, 567–580. doi: 10.1006/jmbi.2000.4315
- Lamour, K. H., Mudge, J., Gobena, D., Hurtado-Gonzales, O. P., Schmutz, J., Kuo, A., et al. (2012). Genome sequencing and mapping reveal loss of heterozygosity as a mechanism for rapid adaptation in the vegetable pathogen *Phytophthora capsici*. *Mol. Plant Microbe Interact.* 25, 1350–1360. doi: 10.1094/MPMI-02-12-0028-R
- Lau, G. W., Chao, C. T., and Ellingboe, A. H. (1993). Interaction of genes controlling avirulence/virulence of *Magnaporthe grisea* on rice cultivar Katy. *Phytopathology* 83, 375–382. doi: 10.1094/Phyto-83-375
- Lawrence, G. J., Mayo, G. M. E., and Shepherd, K. W. (1981). Interactions between genes controlling pathogenicity in the flax rust fungus. *Phytopathology* 71, 12–19. doi: 10.1094/Phyto-71-12
- Le Gac, M., Hood, M. E., Fournier, E., and Giraud, T. (2007). Phylogenetic evidence of host-specific cryptic species in the anther smut fungus. *Evolution* 61, 15–26. doi: 10.1111/j.1558-5646.2007.00002.x
- Lee, S., Garzón, C. D., and Moorman, G. W. (2010). Genetic structure and distribution of *Pythium aphanidermatum* populations in Pennsylvania greenhouses based on analysis of AFLP and SSR markers. *Mycologia* 102, 774–784. doi: 10.3852/09-018
- Leonelli, L., Pelton, J., Schoeffler, A., Dahlbeck, D., Berger, J., Wemmer, D. E., et al. (2011). Structural elucidation and functional characterization of the *Hyaloperonospora arabidopsidis* effector protein ATR13. *PLoS Pathog.* 7:e1002428. doi: 10.1371/journal.ppat.1002428
- Letunic, I., Doerks, T., and Bork, P. (2012). SMART 7, recent updates to the protein domain annotation resource. *Nucleic Acids Res.* 40, D302–D305. doi: 10.1093/nar/gkr931
- Li, W. H. (1984). Retention of cryptic genes in microbial populations. *Mol. Biol. Evol.* 1, 213–219.
- Li, Y., van der Lee, T. A., Evenhuis, A., van den Bosch, G. B., van Bekkum, P. J., Förch, M. G., et al. (2012). Population dynamics of *Phytophthora infestans* in the Netherlands reveals expansion and spread of dominant clonal lineages and virulence in sexual offspring. *G3* 2, 1529–1540. doi: 10.1534/g3.112.004150
- Livak, K. J., and Schmittgen, T. D. (2001). Analysis of relative gene expression data using real-time quantitative PCR and the $2^{-\Delta\Delta C(T)}$ method. *Methods* 25, 402–408. doi: 10.1006/meth.2001.1262
- Luzzatto, L. (2012). Sickle cell anaemia and malaria. *Mediterr. J. Hematol. Infect. Dis.* 4:e2012065. doi: 10.4084/mjhid.2012.065
- McDowell, J. M., Dhandaydham, M., Long, T. A., Aarts, M. G., Goff, S., Holub, E. B., et al. (1998). Intragenic recombination and diversifying selection contribute to the evolution of downy mildew resistance at the RPP8 locus of Arabidopsis. *Plant Cell* 10, 1861–1874. doi: 10.1105/tpc.10.11.1861
- Modiano, G., Ciminelli, B. M., and Pignatti, P. F. (2007). Cystic fibrosis and lactase persistence, a possible correlation. *Eur. J. Hum. Genet.* 15, 255–259. doi: 10.1038/sj.ejhg.5201749
- Na, R., and Gijzen, M. (2016). Escaping host immunity, New tricks for plant pathogens. *PLoS Pathog.* 12:e1005631. doi: 10.1371/journal.ppat.1005631
- Neff, M. M., Turk, E., and Kalishman, M. (2002). Web-based primer design for single nucleotide polymorphism analysis. *Trends Genet.* 18, 613–615. doi: 10.1016/S0168-9525(02)02820-2
- Nemri, A., Atwell, S., Tarone, A. M., Huang, Y. S., Zhao, K., Studholme, D. J., et al. (2010). Genome-wide survey of Arabidopsis natural variation in downy mildew resistance using combined association and linkage mapping. *Proc. Natl. Acad. Sci. U.S.A.* 107, 10302–10307. doi: 10.1073/pnas.0913160107
- Nordborg, M., Hu, T. T., Ishino, Y., Jhaveri, J., Toomajian, C., Zheng, H., et al. (2005). The pattern of polymorphism in *Arabidopsis thaliana*. *PLoS Biol.* 3:e196. doi: 10.1371/journal.pbio.0030196
- Parker, J. E., Holub, E. B., Frost, L. N., Falk, A., Gunn, N. D., and Daniels, M. J. (1996). Characterization of eds1, a mutation in Arabidopsis suppressing resistance to *Peronospora parasitica* specified by several different RPP genes. *Plant Cell* 8, 2033–2046. doi: 10.1105/tpc.8.11.2033
- Pedersen, C., Ver Loren van Themaat, E., McGuffin, L. J., Abbott, J. C., Burgis, T. A., Barton, G., et al. (2012). Structure and evolution of barley powdery mildew effector candidates. *BMC Genomics* 13:694. doi: 10.1186/1471-2164-13-694
- Penn, D. J., Damjanovich, K., and Potts, W. K. (2002). MHC heterozygosity confers a selective advantage against multiple-strain infections. *Proc. Natl. Acad. Sci. U.S.A.* 99, 11260–11264. doi: 10.1073/pnas.162006499
- Petersen, T. N., Brunak, S., von Heijne, G., and Nielsen, H. (2011). SignalP 4.0, discriminating signal peptides from transmembrane regions. *Nat. Methods* 8, 785–786. doi: 10.1038/nmeth.1701
- Punta, M., Coghill, P. C., Eberhardt, R. Y., Mistry, J., Tate, J., Boursnell, C., et al. (2012). The Pfam protein families database. *Nucleic Acids Res.* 40, D290–D301. doi: 10.1093/nar/gkr1065
- Quevillon, E., Silventoinen, V., Pillai, S., Harte, N., Mulder, N., Apweiler, R., et al. (2005). InterProScan, protein domains identifier. *Nucleic Acids Res.* 33, W116–W120. doi: 10.1093/nar/gki442
- Rehmany, A. P., Gordon, A., Rose, L. E., Allen, R. L., Armstrong, M. R., Whisson, S. C., et al. (2005). Differential recognition of highly divergent downy mildew avirulence gene alleles by RPP1 resistance genes from two Arabidopsis lines. *Plant Cell* 17, 1839–1850. doi: 10.1105/tpc.105.031807
- Shan, L., He, P., Li, J., Heese, A., Peck, S. C., Nürnberger, T., et al. (2008). Bacterial effectors target the common signaling partner BAK1 to disrupt multiple MAMP receptor-signaling complexes and impede plant immunity. *Cell Host Microbe* 4, 17–27. doi: 10.1016/j.chom.2008.05.017
- Sinapidou, E., Williams, K., Nott, L., Bahkt, S., Tör, M., Crute, I., et al. (2004). Two TIR: NB:LRR genes are required to specify resistance to *Peronospora parasitica* isolate Calaz₂ in Arabidopsis. *Plant J.* 38, 898–909. doi: 10.1111/j.1365-313X.2004.02099.x

- Sohn, K. H., Lei, R., Nemri, A., and Jones, J. D. (2007). The downy mildew effector proteins ATR1 and ATR13 promote disease susceptibility in *Arabidopsis thaliana*. *Plant Cell* 19, 4077–4090. doi: 10.1105/tpc.107.054262
- Song, J., Win, J., Tian, M., Schornack, S., Kaschani, F., Ilyas, M., et al. (2009). Apoplastic effectors secreted by two unrelated eukaryotic plant pathogens target the tomato defense protease Rcr3. *Proc. Natl. Acad. Sci. U.S.A.* 106, 1654–1659. doi: 10.1073/pnas.0809201106
- Steinbrenner, A. D., Goritschnig, S., and Staskawicz, B. J. (2015). Recognition and activation domains contribute to allele-specific responses of an Arabidopsis NLR receptor to an oomycete effector protein. *PLoS Pathog.* 11:e1004665. doi: 10.1371/journal.ppat.1004665
- Tör, M., Gordon, P., Cuzick, A., Eulgem, T., Sinapidou, E., Mert-Türk, F., et al. (2002). Arabidopsis SGT1b Is required for defense signaling conferred by several downy mildew resistance genes. *Plant Cell* 14, 993–1003. doi: 10.1105/tpc.001123
- Tör, M., Holub, E. B., Brose, E., Musker, R., and Gunn, N. (1994). Map positions of three loci in *Arabidopsis thaliana* associated with isolate-specific recognition of *Peronospora parasitica* (downy mildew). *Mol. Plant Microbe Interact.* 7, 214–222. doi: 10.1094/MPMI-7-0214
- Tyler, B. M., Kale, S. D., Wang, Q., Tao, K., Clark, H. R., Drews, K., et al. (2013). Microbe-independent entry of oomycete RxLR effectors and fungal RxLR-like effectors into plant and animal cells is specific and reproducible. *Mol. Plant Microbe Interact.* 26, 611–616. doi: 10.1094/MPMI-02-13-0051-1A
- van der Biezen, E. A., Freddie, C. T., Kahn, K., Parker, J. E., and Jones, J. D. (2002). Arabidopsis RPP4 is a member of the RPP5 multigene family of TIR-NB-LRR genes and confers downy mildew resistance through multiple signalling components. *Plant J.* 29, 439–451. doi: 10.1046/j.0960-7412.2001.01229.x
- Vinatzer, B. A., Teitzel, G. M., Lee, M. W., Jelenska, J., Hotton, S., Fairfax, K., et al. (2006). The type III effector repertoire of *Pseudomonas syringae* pv. *syringae* B728a and its role in survival and disease on host and non-host plants. *Mol. Microbiol.* 62, 26–44. doi: 10.1111/j.1365-2958.2006.05350.x
- Wawra, S., Trusch, F., Matena, A., Apostolakis, K., Linne, U., Zhukov, I., et al. (2017). The RxLR motif of the host targeting effector AVR3a of *Phytophthora infestans* is cleaved before secretion. *Plant Cell* 29, 1184–1195. doi: 10.1105/tpc.16.00552
- Whisson, S. C., Boevink, P. C., Moleleki, L., Avrova, A. O., Morales, J. G., Gilroy, E. M., et al. (2007). A translocation signal for delivery of oomycete effector proteins into host plant cells. *Nature* 450, 115–118. doi: 10.1038/nature06203
- Whitford, R., Fleury, D., Reif, J. C., Garcia, M., Okada, T., Korzun, V., et al. (2013). Hybrid breeding in wheat, technologies to improve hybrid wheat seed production. *J. Exp. Bot.* 64, 5411–5428. doi: 10.1093/jxb/ert333
- Win, J., Chaparro-Garcia, A., Belhaj, K., Saunders, D. G., Yoshida, K., Dong, S., et al. (2013). Effector biology of plant-associated organisms, concepts and perspectives. *Cold Spring Harb. Symp. Quant. Biol.* 77, 235–247. doi: 10.1101/sqb.2012.77.015933
- Zheng, W., Huang, L., Huang, J., Wang, X., Chen, X., Zhao, J., et al. (2013). High genome heterozygosity and endemic genetic recombination in the wheat stripe rust fungus. *Nat. Commun.* 4, 2673. doi: 10.1038/ncomms3673

Conflict of Interest Statement: The authors declare that the research was conducted in the absence of any commercial or financial relationships that could be construed as a potential conflict of interest.

Copyright © 2018 Woods-Tör, Studholme, Cevik, Telli, Holub and Tör. This is an open-access article distributed under the terms of the Creative Commons Attribution License (CC BY). The use, distribution or reproduction in other forums is permitted, provided the original author(s) and the copyright owner are credited and that the original publication in this journal is cited, in accordance with accepted academic practice. No use, distribution or reproduction is permitted which does not comply with these terms.